

Structure–Stability Relationships of 3-Hydroxypyridin-4-one Complexes†

Gaoyi Xiao,^a Dick van der Helm,^{*a} Robert C. Hider^b and Paul S. Dobbin^b

^a Department of Chemistry and Biochemistry, The University of Oklahoma, Norman, OK 73019, USA

^b Department of Pharmacy, King's College London, London SW3 6LX, UK

The structural features of the ligand 1-ethyl-3-hydroxy-2-methylpyridin-4-one HL¹ and its tris complexes [ML₃] \cdot 3H₂O (M = Fe **1**, Ga **2** and Al **3**) have been characterized by single-crystal X-ray diffraction. The crystal structures of complexes **1–3** are isomorphous. The comparisons among HL¹ and **1–3** indicate that several resonance forms play an important role in determining their structures. It is concluded that the absolute stabilities of the complexes of Al³⁺ and Ga³⁺ are similar and both greater than that of the iron(III) complex. A structural comparison between ligand HL¹ and the closely related 1-butyl-3-hydroxypyridin-2-one provides an explanation for the higher affinity of 3-hydroxypyridin-4-ones for Fe³⁺ over 3-hydroxypyridin-2-ones. The complexes of Al³⁺ and Ga³⁺ with HL¹ can be crystallized both as tri- and dodeca-hydrates. It is shown by comparing the same complex in different environments that neither the interplanar angle nor the twist angle is a reliable structural parameter to characterize a metal complex.

There is a considerable demand for clinically useful, orally active, iron(III) chelators.^{1,2} Such compounds would find application in the treatment of iron overload in transfusion-dependent thalassaemia patients³ and possibly for the treatment of a range of symptoms caused by iron-induced radical formation.⁴ 1-Ethyl-3-hydroxy-2-methylpyridin-4-one HL¹ is one of a small number of promising synthetic chelators which have potential for this purpose.⁵ A systematic crystallographic study on this ligand and its complexes [ML₃]⁺ (M = Fe **1**, Ga **2** or Al **3**) was initiated because we believed that the results would enhance the understanding of the affinity and specificity of the ligand for Fe³⁺ and other trivalent metal ions. The structures of the closely related 1-butyl-3-hydroxypyridin-2-one and its iron(III) trihydrate complex have been reported.⁶ Structural comparisons between these ligands and also between their tris complexes with Fe³⁺ can provide an explanation for the higher affinity of 3-hydroxypyridin-4-ones for Fe³⁺ over 3-hydroxypyridin-2-ones.

The structures of a number of natural hydroxamate siderophores have been determined,⁷ but their accuracy is limited due to the large molecular size. The structures of smaller model hydroxamic acids and their iron(III) complexes have allowed the opportunity to relate thermodynamic stability with bond distances and their differences.^{8–10} In addition it has been possible to make similar geometric comparisons between the complexes of Fe³⁺ and Ga³⁺ of a particular hydroxamic acid and make qualitative conclusions regarding their stability constants.¹¹ The present paper reports a similar study on 1-ethyl-3-hydroxy-2-methylpyridin-4-one.

The metal complexes of this ligand can be crystallized both as tri- and dodeca-hydrates. The structures of the dodecahydrates of Ga³⁺ and Al³⁺ at room temperature have been published.¹² The present study of [ML₃] \cdot 3H₂O (M = Fe **1**, Ga **2** or Al **3**) allows a unique opportunity to compare the structures of the same complex in different environments. The structure of the ligand at room temperature has been reported earlier¹² but the

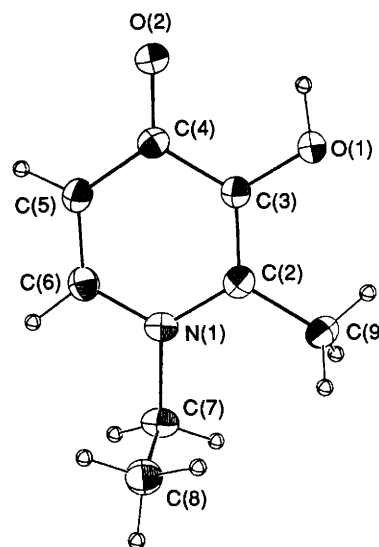


Fig. 1 An ORTEP drawing of ligand HL¹

present structure at low temperature is more accurate ($R = 0.034$ vs. 0.053) and allows for better comparison with the metal(III) trihydrate complexes. Also the structures of tris(3-hydroxy-1,2-dimethylpyridin-4-one) dodecahydrate complexes with Fe³⁺,¹³ Al³⁺ and Ga³⁺¹⁴ are known. Recently, the complexes of Al³⁺ and Ga³⁺ with 3-hydroxy-2-methyl-1-propylpyridin-4-one and that of Al³⁺ with 1-butyl-3-hydroxy-2-methylpyridin-4-one were reported.¹⁵ These structures proved to be trihydrates.

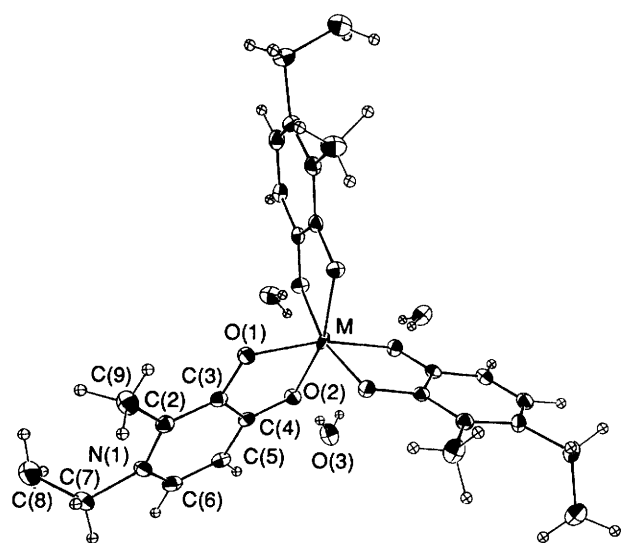
Results and Discussion

General Description of the Structures.—The ORTEP plots of a single molecule of the ligand ML¹ and of one of its metal complexes are shown in Figs. 1 and 2 together with the numbering scheme. Bond distances, angles and selected torsion angles are presented in Table 1.

† Supplementary data available: see Instructions for Authors, *J. Chem. Soc., Dalton Trans.*, 1992, Issue 1, pp. xx–xxv.

Table 1 Bond distances (Å), angles and selected torsion angles (°) for compounds HL¹ and 1–3

	HL ¹	1	2	3
M–O(1)		1.995(1)	1.964(1)	1.893(1)
M–O(2)		2.035(1)	1.987(1)	1.916(1)
O(1)–C(3)	1.356(1)	1.332(2)	1.336(2)	1.333(2)
O(2)–C(4)	1.265(1)	1.307(2)	1.310(2)	1.307(2)
C(3)–C(4)	1.442(2)	1.429(3)	1.426(2)	1.421(2)
N(1)–C(2)	1.380(1)	1.379(3)	1.384(2)	1.379(2)
N(1)–C(6)	1.358(2)	1.357(3)	1.354(3)	1.359(2)
N(1)–C(7)	1.480(1)	1.483(3)	1.479(2)	1.479(2)
C(2)–C(3)	1.370(2)	1.384(3)	1.385(2)	1.380(2)
C(2)–C(9)	1.494(2)	1.491(3)	1.494(4)	1.497(3)
C(4)–C(5)	1.418(2)	1.402(3)	1.400(2)	1.396(3)
C(5)–C(6)	1.359(2)	1.366(3)	1.375(2)	1.367(3)
C(7)–C(8)	1.511(2)	1.515(2)	1.521(3)	1.512(2)
M–O(1)–C(3)		113.3(1)	111.3(1)	112.7(1)
M–O(2)–C(4)		112.8(1)	111.6(1)	112.2(1)
O(1)–M–O(2)		80.37(5)	82.93(5)	83.96(5)
O(1)–C(3)–C(2)	118.8(1)	123.5(2)	123.0(2)	124.4(2)
O(1)–C(3)–C(4)	118.71(9)	116.1(2)	116.6(1)	115.2(1)
O(2)–C(4)–C(3)	121.0(1)	116.6(2)	116.9(1)	115.2(1)
O(2)–C(4)–C(5)	124.2(1)	125.0(2)	124.4(2)	125.6(2)
N(1)–C(2)–C(3)	119.1(1)	118.7(2)	118.5(2)	118.5(2)
N(1)–C(2)–C(9)	119.2(1)	119.9(2)	119.8(1)	119.7(2)
N(1)–C(6)–C(5)	121.8(1)	122.1(2)	121.9(2)	122.3(2)
N(1)–C(7)–C(8)	116.6(1)	111.8(2)	112.1(2)	112.4(2)
C(2)–N(1)–C(6)	120.43(9)	121.2(2)	121.4(1)	121.1(1)
C(2)–N(1)–C(7)	121.96(9)	121.7(2)	121.4(2)	121.7(2)
C(6)–N(1)–C(7)	117.41(9)	117.1(2)	117.2(1)	117.2(2)
C(2)–C(3)–C(4)	122.5(1)	120.4(2)	120.4(2)	120.4(2)
C(3)–C(2)–C(9)	121.7(1)	121.4(2)	121.6(2)	121.8(2)
C(3)–C(4)–C(5)	114.7(1)	118.4(2)	118.7(2)	119.2(1)
C(4)–C(5)–C(6)	121.5(1)	119.1(2)	118.9(2)	118.3(2)
M–O(1)–C(3)–C(2)		171.8(1)	171.7(2)	–171.3(1)
M–O(1)–C(3)–C(4)		–8.1(2)	–8.2(2)	8.1(1)
M–O(2)–C(4)–C(3)		4.8(1)	3.4(2)	–2.8(1)
M–O(2)–C(4)–C(5)		–174.4(1)	–175.6(2)	176.2(1)
O(1)–M–O(2)–C(4)		–6.96(9)	–6.1(1)	5.74(8)
O(2)–M–O(1)–C(3)		8.1(1)	7.8(1)	–7.58(9)
O(1)–C(3)–C(4)–O(2)	0.3(2)	2.2(2)	3.3(3)	–3.5(2)

**Fig. 2** An ORTEP drawing for one of the metal trihydrate complexes [ML³⁺]₃·3H₂O (M = Fe, Ga or Al)

The crystal structure of the ligand is the same as previously observed.¹² The molecules form centrosymmetric hydrogen-bonded pairs with only van der Waals forces between dimers as found for the NH and NMe derivatives of the 3-hydroxy-2-methylpyridin-4-ones.¹⁶

The crystal structures of the three complexes [ML³⁺]₃·3H₂O (M = Fe, Ga or Al) are isostructural. The metal atom occupies a position on the three-fold axis and is co-ordinated to six O atoms from three facial (three-fold-related) ligands, forming a distorted octahedron. All six chelating O atoms are hydrogen bonded to the three H₂O molecules related by a three-fold axis. They form bridges from the hydroxy O(1) in one ligand to the carbonyl O(2) of a ligand rotated by 120° and translated by one *c* unit, giving the appearance of an infinite prism down the three-fold *c* axis as shown in Fig. 3. The same packing arrangement is found in the complexes of Al³⁺ and Ga³⁺ with 3-hydroxy-2-methyl-1-propylpyridin-4-one, and the complex of Al³⁺ with 1-butyl-3-hydroxy-2-methylpyridin-4-one, which also crystallized as trihydrates.¹⁵ There are no hydrogen bonds parallel to the *ab* plane and the molecules are held together only by van der Waals forces in this plane. The hydrogen bonds involving carbonyl O(2) atoms are consistently stronger than those involving hydroxyl O(1) atoms in all the three complexes (Table 2) despite the fact that the hydroxyl oxygen atom O(1) carries more negative charge to form a stronger M–O bond than the carbonyl oxygen atom O(2). This observation may be explained by considering that the negative charge on the hydroxy O(1) atom is less available to form a hydrogen bond than that on the carbonyl O(2) atom.

Effect of the Environment on Structural Parameters of Complexes of 1-ethyl-3-hydroxy-2-methylpyridin-4-one.—The present structure determinations of the trihydrate complexes and the previously determined structures of the dodecahydrate complexes¹² allow a unique opportunity to compare the

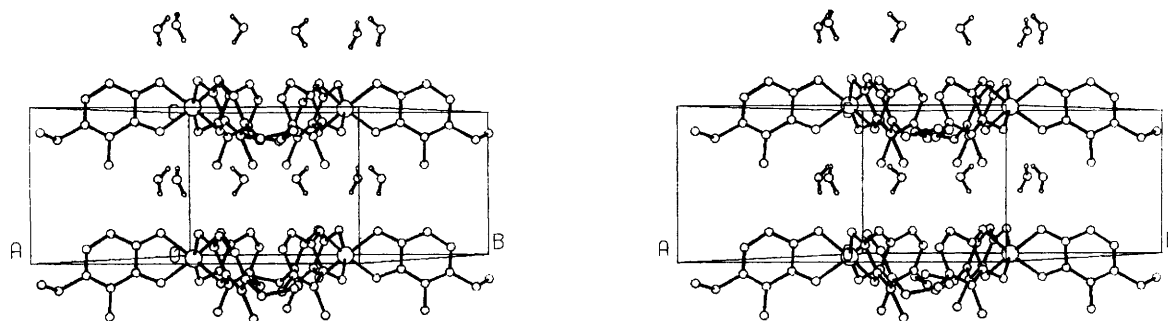


Fig. 3 Stereoview of the crystal packing for one of the metal trihydrate complexes $[ML^1_3] \cdot 3H_2O$

Table 2 Hydrogen-bond distances (Å) and angles (°)

	O...O			O-H...O		
	1	2	3	1	2	3
O(w)-H...O(1)	2.989	2.954	2.939	152	155	150
O(w)-H...O(2)	2.825	2.820	2.826	168	166	162

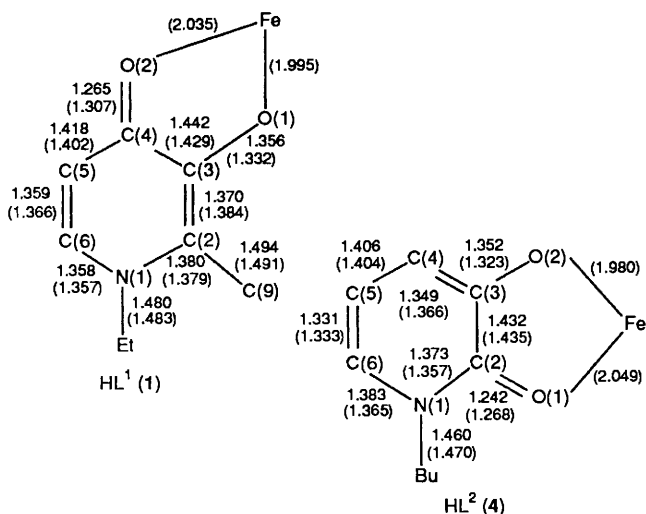
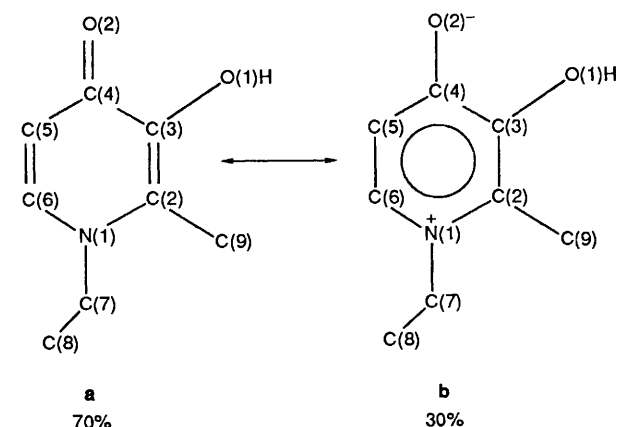


Fig. 4 Bond distances in HL^1 and its iron(III) complex 1 (in parentheses) and HL^2 and its iron(III) complex 4 (in parentheses)

structures of the same complex (Ga^{3+} and Al^{3+}) in different environments. Selected geometric values for the tri- and dodecahydrate complexes are calculated and listed in Table 3. It is observed that the trihydrate complexes have smaller cell volumes than the corresponding dodecahydrate complexes, as expected, but that quite unexpectedly the c axes of the former are longer than those for the dodecahydrate complexes. Within one series, *i.e.* either the tri- or dodecahydrate structures, one observes similar trends: decreasing interplanar angles and increasing ligand bites and twist angles going from Fe^{3+} (in the case of the trihydrate) to Ga^{3+} to Al^{3+} . If one, however, focuses on a particular metal ion, only the ligand bite is constant and both the interplanar angles and the twist angles are variable for a particular complex. Therefore these last two parameters are easily affected by the environment of a metal complex.

Comparison of 3-Hydroxypyridin-2-one with a 3-Hydroxypyridin-4-one as Ligands for Metal Complexation.—All four structures have been determined quite accurately with standard deviations of 0.001–0.002 Å for the ligand and 0.001–0.003 Å for the complexes. It should therefore be possible to make certain conclusions about both the ligand and the complexes based on the observed geometries of the molecules.



Scheme 1 Two resonance forms **a** and **b** of the free ligand HL^1 and their estimated contributions

The bond distances in the free ligand HL^1 are shown in Fig. 4 and they compare well with those reported by Nelson *et al.*¹² They also agree with those observed for the *N*-methyl derivative.^{16,17} This implies that the alkyl substituents on the nitrogen atom have little effect on both the ring and the 3 and 4 substituents of the ring. In the structure of HL^1 the C(4)–O(2) bond is significantly shorter than the C(3)–O(1) bond, indicating a contribution from resonance form **a** shown in Scheme 1. On the other hand, the C(4)–O(2) bond is considerably longer (1.265 Å) than a pure ketone bond (1.210 Å). This provides the O(2) atom with a partial negative charge and hence resonance form **b** (see Scheme 1) is important as well. As a consequence, the N atom carries a partial positive charge. The relative contributions for resonance forms **a** and **b** are estimated from bond-length comparisons and indicated in Scheme 1. It is obvious that the resonance form **b** is in part responsible for the high affinity of the 3-hydroxypyridin-4-one molecule for iron(III) and other metal(III) ions.

The 3-hydroxypyridin-2-ones form similar complexes and it is therefore useful to compare the structures of these ligands with those of 3-hydroxypyridin-4-ones. This is done in Fig. 4 where the bond distances in HL^1 are compared with those in 1-butyl-3-hydroxypyridin-2-one HL^2 .⁶ The most obvious difference is found in the carbonyl bond distance which is 0.023 Å shorter in HL^2 . It can be therefore concluded that a resonance form similar to **b** in Scheme 1 is of less importance in HL^2 and hence a smaller negative charge resides on the carbonyl oxygen atom in HL^2 compared to HL^1 . This observation offers an explanation for the finding that the 2-pyridone ligands form less-stable metal complexes with tribasic cations than do the 4-pyridone ligands.¹⁸

Structural Changes in the Ligand upon Chelation.—It is anticipated that upon metal-ion chelation the hydroxyl oxygen atom O(1) will be deprotonated and the negative charge on this atom will be delocalized through resonance extending from

Table 3 Selected geometry values for the metal chelate tri- and dodeca-hydrates

M	U/Å ³		c/Å		Interplanar angle (°) ^a		Ligand bite ^b		Twist angle (°) ^c	
	Trihydrate	Dodeca-hydrate	Trihydrate	Dodeca-hydrate	Trihydrate	Dodeca-hydrate	Trihydrate	Dodeca-hydrate	Trihydrate	Dodeca-hydrate
Fe	1395.2(8)		7.140(2)		101.47(5)		1.29(1)		41.8(1)	
Ga	1383.1(6)	1759.4(3)	7.115(1)	6.830(1)	99.24(4)	95.54(4)	1.32(1)	1.33(1)	46.2(1)	49.6(1)
Al	1366.6(3)	1743.7(5)	7.081(1)	6.827(2)	98.13(5)	95.07(3)	1.34(1)	1.34(1)	48.0(1)	50.8(1)

^a Formed between the five-membered metal chelate rings. ^b Ratio of the average O(1)···O(2) distance to the average Fe–O distance. ^c Angle of rotation of O(1)–O(1')–O(1'') face of co-ordination with respect to O(2)–O(2')–O(2'') face. The primes indicate the other two three-fold symmetry-related chelating oxygen atoms.

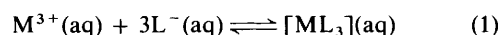
O(1) to O(2) via C(3) and C(4) atoms. On the other hand, the carbonyl oxygen atom O(2) will withdraw more electrons through the C(4)–O(2) bond when forming a bond with a metal ion with high positive charge density. As a consequence, there will be a shortening of the O(1)–C(3) and C(3)–C(4) bonds and a lengthening of the C(4)–O(2) bond. All of these dimensional changes are indeed observed. The bond distance changes for the complex of Fe³⁺ are also presented in Fig. 4. The Fe–O distances observed are quite similar to those observed in the iron(III) complex of the 1,2-dimethyl derivative.¹³ The C(4)–O(2) bond becomes significantly longer by 0.042, 0.045 and 0.042 Å in **1**, **2** and **3**, respectively. Meanwhile, the C(3)–C(4) bond decreases in length by 0.013, 0.016 and 0.021 Å, respectively. Metal-ion chelation brings about a shortening of the C(3)–O(1) bond by 0.024, 0.020 and 0.023 Å, respectively. There is a significant averaging of the single bonds, C(3)–C(4) and C(4)–C(5), and the double bonds, C(2)=C(3) and C(5)=C(6), in the ring upon chelation. It is obvious, therefore, that the π delocalization is enhanced by metal chelation. On the other hand, the bond distances involving the N atom remain quite constant when compared to those in the free ligand, indicating that the partial positive charge on the nitrogen atom present in the ligand remains on this atom upon chelation. It also means that more than one electron is distributed over the chelate ring O(1)–C(3)–C(4)–O(2) part of the ligand and thereby accounts for the remarkable strength of the 3-hydroxypyridin-4-one complexes.

Comparison of Iron(III) Complexes of a 3-Hydroxypyridin-4-one with a 3-Hydroxypyridin-2-one.—It is interesting to observe the structural changes which occur when ligand HL² forms the complex [FeL₂]³⁻ **4**⁶ and to compare these with the results of ligand HL¹ and its iron(III) complex **1** (Fig. 4). The qualitative changes in HL² upon chelation to form **4** are similar to those observed in HL¹ and **1**, in that the carbonyl bond lengthens and the hydroxyl bond shortens. However, if complexes **1** and **4** are compared there are obvious differences. In **1** the carbonyl bond is longer by 0.039 Å than the same bond in **4**. Also the difference in the two Fe–O bonds is only 0.040 Å in **1** but 0.069 Å in **4**. Both observations are clear indicators that complex **1** is more stable than **4**, which confirms the conclusion deduced from the comparison of the ligands HL¹ and HL².

Structural Differences between the Isomorphous Complexes of Fe³⁺, Ga³⁺ and Al³⁺ with HL¹ and Qualitative Determination of the Relative Stability of the Complexes.—In these ionic complexes in which crystal-field stabilization is of little significance one can expect the metal ion with the highest charge density to form the most stable complex. Therefore Al³⁺ should form a more stable complex than Ga³⁺ which, in turn, should form a more stable complex than Fe³⁺. This same trend should also be observable in the bond distances when the three complexes are compared. One may expect a more equal distribution of charges over the oxygen atoms which form the chelate bonds to the metal ion for the most stable complex. This effect would be reflected in an increase in the degree of

conjugation of the O(1)–C(3)–C(4)–O(2) bonding system and in a decrease in the C(3)–C(4) bond distance. This distance does indeed decrease in going from the complex of Fe³⁺ to that of Ga³⁺ and of Al³⁺ (Table 4) but the effect is small. The more equal distribution of charges in the strongest complex would make the two M–O distances more equal and this effect is quite obvious (Table 4) in the fact that the difference [$\Delta(M-O)$] becomes smaller on going from Fe³⁺ to Ga³⁺. However, this parameter is the same for the complex of Al³⁺ as it is for that of Ga³⁺. Similarly the difference in the distance of the metal ion to the plane formed by the O(1) atoms compared to the plane formed by the O(2) atoms should become smaller with increasing affinity and again this effect [$\Delta(M-O_{\text{face}})$] is clear for the complex of Ga³⁺ compared to that of Fe³⁺, but the trend is not continued for Al³⁺. These criteria which were previously applied to compare hydroxamate complexes¹¹ lead therefore to the conclusion that the structural stabilities of metal(III) 3-hydroxypyridin-4-onate complexes follow the order Al³⁺ \approx Ga³⁺ > Fe³⁺. The reason that Al³⁺ does not follow the continuing trend observed for Fe³⁺ and Ga³⁺ is believed to be due to its small size, which contracts the size of the octahedral oxygen-atom surroundings to such an extent that repulsive non-bonded O···O interactions between oxygen atoms in different chelate groups destabilize the complex to some extent. It is shown in Table 4 that this is indeed the case by considering the much shorter Al–O bond distances.

Relationship between the Relative Stability of the Complexes and their Formation Constants (β_3).—The formation of the tris(3-hydroxypyridin-4-onate) metal(III) complexes in solution is given by reaction (1), described by the overall formation



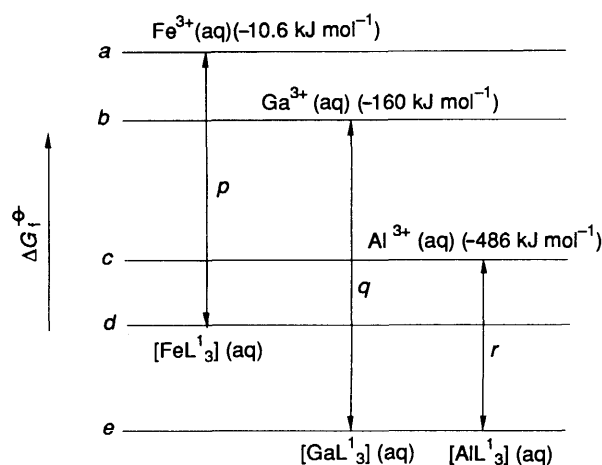
constant [equation (2)]. The latter has been determined

$$\beta_3 = [ML_3]/[M^{3+}][L^{-}]^3 \quad (2)$$

experimentally to be 1.6×10^{38} , 7.9×10^{36} and 1.6×10^{32} dm⁹ mol⁻³ for the tris(2-ethyl-3-hydroxy-1-methylpyridin-4-onate) complexes of Ga³⁺, Fe³⁺ and Al³⁺, respectively,^{19,20} giving the order Ga³⁺ > Fe³⁺ > Al³⁺. There is a proper explanation for the apparent contradiction of structural stabilities with overall formation constants regarding these complexes. Qualitatively, the apparent conflict is explained by realizing that the thermodynamic observations measure the relative values of the standard free energies of formation of both the complex and the constituent ions (metal and ligand), while the structural arguments make conclusions about the stabilities of the complexes themselves. A more quantitative explanation is given in Fig. 5. The overall formation constant of a complex is proportional to the difference in the standard free energies of formation between the aquated complex and metal ion, the ligand being the same in the three complexes. The complexes [ML₃] (M = Fe, Ga or Al) are isomorphous structures, and therefore their entropies are closely similar. The greater

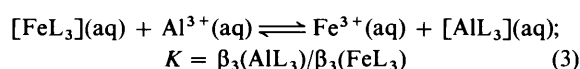
Table 4 Selected bond distances (Å) and angles (°)

Complex	M–O(1)	M–O(2)	Δ(M–O)	Δ[M–O(face)]	C(3)–C(4)	O(1)–M–O(2)	O(1)⋯O(2)
1	1.995(1)	2.035(1)	0.040(1)	0.057(1)	1.429(3)	80.37(5)	2.601(2)
2	1.964(1)	1.987(1)	0.023(1)	0.039(1)	1.426(2)	82.93(5)	2.618(2)
3	1.893(1)	1.916(1)	0.023(1)	0.039(1)	1.421(2)	83.96(5)	2.547(2)

**Fig. 5** Schematic drawing of the relative energy levels of aquated and complexed Fe^{3+} , Ga^{3+} and Al^{3+}

structural stabilities of the complexes of Ga^{3+} and Al^{3+} can be translated into larger (more negative) values of the ΔG_f° for $[\text{GaL}_3]$ and $[\text{AlL}_3]$ (point *e* in Fig. 5) than for $[\text{FeL}_3]$ (point *d* in Fig. 5), assuming that the ΔG_f° is the same for both Ga^{3+} and Al^{3+} . This is based on the conclusion made about the relative structural stabilities of the three complexes. It is not possible to make a quantitative determination of *d* and *e*. The standard free energies of formation for the aqueous metal ions are known²¹ $\{\Delta G_f^\circ[\text{Fe}^{3+}(\text{aq})] = -10.6$, $\Delta G_f^\circ[\text{Ga}^{3+}(\text{aq})] = -159$ and $\Delta G_f^\circ[\text{Al}^{3+}(\text{aq})] = -490$ $\text{kJ mol}^{-1}\}$ and these are indicated in Fig. 5 by levels *a*, *b* and *c* respectively. The lengths of the vectors *p*, *q* and *r* are directly proportional to $\log \beta_3$ and therefore to β_3 of the three complexes. The difference between *d* and *e* is more than compensated for by the much larger differences in free energy of formation of the aqueous ions Fe^{3+} and Al^{3+} , resulting in $|p| > |r|$. It is also obvious that $|q| > |r|$ since $\Delta G_f^\circ[\text{Al}^{3+}(\text{aq})]$ is much more negative than $\Delta G_f^\circ[\text{Ga}^{3+}(\text{aq})]$ and the complexes $[\text{GaL}_3]$ and $[\text{AlL}_3]$ are equally stable. Furthermore, if it is assumed that the difference between the standard free energies of formation of $\text{Fe}^{3+}(\text{aq})$ and $\text{Ga}^{3+}(\text{aq})$ is not great enough to compensate for the larger difference between the free energies of $[\text{FeL}_3]$ and $[\text{GaL}_3]$, then $|q| > |p|$. Therefore, we conclude that $|q| > |p| > |r|$ and as a consequence the overall formation constants of the complexes are in the order of $\beta_3(\text{GaL}_3) > \beta_3(\text{FeL}_3) > \beta_3(\text{AlL}_3)$ which agrees with the experimental observations. It is, therefore, the much lower free energy of the formation of $\text{Al}^{3+}(\text{aq})$ compared to $\text{Fe}^{3+}(\text{aq})$ which determines that the β_3 value of the $[\text{AlL}_3]$ complex is the smallest despite the larger structural stability of the complex.

An understanding of the difference between the absolute stability of a complex and the formation constant, explained above, allows an understanding of the difficulty in making a ligand specific for Al^{3+} compared to Fe^{3+} . A ligand which is more specific for Al^{3+} than for Fe^{3+} requires that $\beta_3(\text{AlL}_3) > \beta_3(\text{FeL}_3)$ because these values determine the equilibrium (3). A large value of $\beta_3(\text{AlL}_3)$ is virtually impos-



sible, however, because the standard free energy of formation for $\text{Al}^{3+}(\text{aq})$ is so much more negative than for $\text{Fe}^{3+}(\text{aq})$ (Fig. 5). It is therefore quite unlikely that one will find a ligand forming a tris complex for which the overall formation constant β_3 is larger for Al^{3+} than for Fe^{3+} and thus being specific for the Al^{3+} ion.

Conclusion

Comparisons of the structural results for 1-ethyl-3-hydroxy-2-methylpyridin-4-one and its trihydrate complexes with Fe^{3+} , Ga^{3+} and Al^{3+} , reported here, together with those for dodecahydrate complexes of Ga^{3+} and Al^{3+} determined earlier¹² allow a number of conclusions.

(1) The twist angle and interplanar angle for a particular complex are affected by the environment of the complex in the solid state and can therefore not be considered to be accurate structural parameters.

(2) The 3-hydroxypyridin-4-one ligand has the characteristics (as judged by the C–O bond lengths) to form more stable metal(III) complexes than those of 3-hydroxypyridin-2-one. This observation is confirmed by the structures of the iron(III) complexes of the two ligands.

(3) The geometric results indicate that the structural stability of the metal complexes of 1-ethyl-3-hydroxy-2-methylpyridin-4-one to be in the order $[\text{FeL}_3] < [\text{GaL}_3] \approx [\text{AlL}_3]$. However, if one takes into account the relative standard free energies of the aqueous ions, it is concluded that the relative values of the formation constant (β_3) to be in the order $[\text{GaL}_3] > [\text{FeL}_3] > [\text{AlL}_3]$, in agreement with the values for these constants observed in aqueous solution.

(4) The very large negative value of the standard free energy of the aqueous Al^{3+} ion makes it virtually impossible to design a bidentate ligand forming a neutral tris complex for which the complex formation constant for Al^{3+} is larger than that for Fe^{3+} .

Experimental

Preparation.—The chemical synthesis of ligand HL^1 has been described elsewhere.²² The complexes 1–3 were prepared from the reaction of the ligand (3 equivalents) with the corresponding metal nitrates, $\text{M}(\text{NO}_3)_3$ ($\text{M} = \text{Fe}, \text{Ga}$ or Al), in the presence of sodium hydroxide. The nitrate (0.667 mmol) dissolved in water (1.00 cm^3) was added dropwise for 10 min to HL^1 (2.00 mmol) dissolved in MeOH (3.00 cm^3). The reaction took place at pH 8.0, adjusted by adding 0.10 mol dm^{-3} NaOH, at 80 °C for 4 h. The complexes were applied to a 1.5×19 cm column of Sephadex LH-20 and eluted with MeOH. The complexes can be crystallized either as trihydrates from non-aqueous solvents or as dodecahydrates from aqueous solvents.

Colourless, rod-shaped crystals of the ligand HL^1 were grown from an ethanol solution equilibrated with heptane at room temperature, and complexes 1–3 were crystallized from dimethylformamide equilibrated with heptane at 0 °C to yield pink-red rods for 1, colourless rods for 2 and colourless rods for 3.

X-Ray Crystallography.—All data were obtained on an Enraf-Nonius CAD-4 diffractometer equipped with a liquid-nitrogen low-temperature device. The crystal and intensity data for all four compounds are given in Table 5. Cell parameters in

Table 5 Crystal and intensity data collection parameters and final refinement results for HL¹ and complexes 1–3*

	HL ¹	1	2	3
Formula	C ₈ H ₁₁ NO ₂	C ₂₄ H ₃₀ FeN ₃ O ₆ ·3H ₂ O	C ₂₄ H ₃₀ GaN ₃ O ₆ ·3H ₂ O	C ₂₄ H ₃₀ AlN ₃ O ₆ ·3H ₂ O
Crystal size/mm	0.60 × 0.20 × 0.20	0.30 × 0.10 × 0.10	0.30 × 0.10 × 0.15	0.20 × 0.05 × 0.05
Crystal system	Orthorhombic	Trigonal	Trigonal	Trigonal
Space group	<i>Pbca</i>	<i>P</i> $\bar{3}$	<i>P</i> $\bar{3}$	<i>P</i> $\bar{3}$
<i>a</i> /Å	11.108(2)	15.021(3)	14.982(2)	14.928(1)
<i>b</i> /Å	12.390(1)			
<i>c</i> /Å	11.569(1)	7.140(2)	7.115(1)	7.081(1)
<i>U</i> /Å ³	1588.3(5)	1395.2(8)	1383.1(6)	1366.6(3)
<i>Z</i>	8	2	2	2
<i>D_c</i> /g cm ⁻³	1.28	1.35	1.39	1.31
Radiation	Cu-K α	Mo-K α	Mo-K α	Cu-K α
μ /cm ⁻¹	6.10	5.43	11.95	7.43
<i>F</i> (000)	656	592	602	566
$2\theta_{\max}$ /°	150	53	53	150
Scan width/°	0.80 + 0.20 tan θ	0.85 + 0.35 tan θ	0.85 + 0.20 tan θ	0.80 + 0.20 tan θ
Horizontal aperture/mm	4.0 + 0.86 tan θ	3.5 + 0.86 tan θ	3.5 + 0.86 tan θ	3.5 + 0.86 tan θ
Total measurements	1626	1915	1901	2163
No. observed reflections [<i>I</i> ≥ 2σ(<i>I</i>)]	1480	1559	1648	1455
<i>R</i>	0.034	0.037	0.029	0.037
<i>R'</i>	0.053	0.041	0.037	0.041

* Details in common: vertical aperture 6.0 mm; scan technique θ –2 θ ; 132(2) K; $w = 1/\sigma_F^2$ where σ_F^2 was from counting statistics; t_{\max} 90 s.

Table 6 Fractional atomic coordinates (× 10⁴) for ligand HL¹

Atom	<i>x</i>	<i>y</i>	<i>z</i>
O(1)	1391.6(7)	3818.9(7)	5327.0(7)
O(2)	746.3(7)	5526.9(7)	3944.5(7)
N(1)	4179.0(8)	4358.9(8)	3839.3(8)
C(2)	3351(1)	3886.5(9)	4570.9(9)
C(3)	2202.1(9)	4288.1(9)	4608.9(9)
C(4)	1817(1)	5180.8(9)	3899.6(9)
C(5)	2715(1)	5598.7(9)	3153(1)
C(6)	3849(1)	5186.9(9)	3139(1)
C(7)	5417(1)	3933(1)	3711(1)
C(8)	5492(1)	3095(1)	2765(1)
C(9)	3731(1)	2957(1)	5308(1)

Table 7 Fractional atomic coordinates (× 10⁴) for complex 1

Atom	<i>x</i>	<i>y</i>	<i>z</i>
Fe	3333.3	6666.7	144.1(8)
O(1)	2510(1)	5425(1)	–1439(2)
O(2)	2074(1)	5894(1)	1808(2)
O(3)	1542(1)	6301(1)	5374(3)
N(1)	–151(1)	3415(1)	–998(3)
C(9)	1024(2)	3710(2)	–3672(3)
C(2)	812(1)	3985(1)	–1783(3)
C(3)	1560(1)	4819(1)	–799(3)
C(4)	1337(1)	5075(1)	1001(3)
C(5)	355(1)	4448(1)	1758(3)
C(6)	–362(1)	3640(1)	729(3)
C(7)	–999(2)	2532(2)	–1995(4)
C(8)	–1036(2)	1530(2)	–1530(4)

Table 8 Fractional atomic coordinates (× 10⁴) for complex 2

Atom	<i>x</i>	<i>y</i>	<i>z</i>
Ga	6 666.7	3 333.3	10 153.6(6)
O(1)	7 122(1)	2 562(1)	8 570(2)
O(2)	6 151(1)	2 098(1)	11 792(2)
O(3)	5 252(1)	1 526(1)	15 391(3)
N(1)	6 456(1)	–112(1)	9 014(3)
C(9)	7 360(2)	1 073(2)	6 340(4)
C(2)	6 861(2)	860(2)	8 231(3)
C(3)	6 763(2)	1 605(2)	9 212(3)
C(4)	6 260(1)	3 171(2)	10 994(3)
C(5)	5 905(2)	390(2)	11 760(4)
C(6)	6 010(2)	–330(2)	10 733(4)
C(7)	6 492(2)	–957(2)	8 005(4)
C(8)	7 459(2)	–1 004(2)	8 475(5)

Table 9 Fractional atomic coordinates (× 10⁴) for complex 3

Atom	<i>x</i>	<i>y</i>	<i>z</i>
Al	6 666.7	3 333.3	9 838(1)
O(1)	7 395.4(9)	4 522.1(9)	11 373(2)
O(2)	7 861.9(9)	4 012.1(9)	8 248(2)
O(3)	8 451(1)	3 740(1)	14 595(2)
N(1)	10 075(1)	6 549(1)	10 975(2)
C(9)	8 883(2)	6 275(2)	13 647(3)
C(2)	9 101(1)	5 982(1)	11 751(3)
C(3)	8 360(1)	5 137(1)	10 770(3)
C(4)	8 601(1)	4 862(1)	8 998(3)
C(5)	9 581(1)	5 486(1)	8 219(3)
C(6)	10 294(1)	6 310(1)	9 249(3)
C(7)	10 926(1)	7 430(1)	11 988(3)
C(8)	10 977(2)	8 445(2)	11 545(4)

each case were obtained by a least-squares fit to 48 reflections from all of the reciprocal space. For each compound the data were corrected for Lorentz and polarization factors, but no absorption correction was made. The structure of HL¹ was solved by direct methods using SHELX 76,²³ those of 1 and 2 by Patterson vector methods while for 3 the structure of 1 was used as a model. In the complexes the metal atoms were in special positions with constrained anisotropic thermal parameters. In all cases, the non-hydrogen atoms were refined anisotropically; all the H atoms were located on Fourier difference maps and refined isotropically, using SHELXS 86.²⁴ The drawings of the complexes were made with ORTEP.²⁵ The final refinement results are listed in Table 5. The atomic coordinates of the non-

hydrogen atoms for the ligand HL¹ and complexes 1, 2 and 3 are listed in Tables 6, 7, 8 and 9, respectively.

Additional material available from the Cambridge Crystallographic Data Centre comprises H-atom coordinates, thermal parameters and remaining bond lengths and angles.

Acknowledgements

Financial support of this work by a grant from the National Institute for General Medical Sciences (GM-21822) is gratefully acknowledged.

References

- 1 A. E. Martell, W. F. Anderson and D. G. Badman, *Development of Iron Chelators for Clinical Use*, Elsevier/North Holland, New York, 1981.
- 2 J. B. Porter, R. C. Hider and E. R. Huehns, in *Semin. Hematol.*, 1990, **27**, 95.
- 3 D. J. Weatherall, M. J. Pippard and S. T. Callender, *New Eng. J. Med.*, 1983, **308**, 456.
- 4 C. Herskho, *Br. Med. J.*, 1988, **296**, 1081.
- 5 E. R. Huehns, J. B. Porter and R. C. Hider, *Hemoglobin*, 1988, **12**, 593.
- 6 R. C. Scarrow and K. N. Raymond, *Inorg. Chem.*, 1988, **27**, 4140.
- 7 D. van der Helm, M. A. Jalal and M. B. Hossain, in *Iron Transport in Microbes, Plants and Animals*, eds. G. Winkelmann, D. van der Helm and J. B. Neilands, VCH, New York, 1987, p. 135.
- 8 R. Mocharla, D. R. Powell, C. L. Barnes and D. van der Helm, *Acta Crystallogr., Sect. C*, 1983, **39**, 868.
- 9 R. Mocharla, D. R. Powell and D. van der Helm, *Acta Crystallogr., Sect. C*, 1984, **40**, 1369.
- 10 D. R. Powell and D. van der Helm, *Acta Crystallogr., Sect. C*, 1987, **43**, 493.
- 11 A. Dietrich, K. A. Fidelis, D. R. Powell, D. van der Helm and D. L. Eng-Wilmot, *J. Chem. Soc., Dalton Trans.*, 1991, 231.
- 12 W. O. Nelson, S. J. Rettig and C. Orvig, *Inorg. Chem.*, 1989, **28**, 3153.
- 13 J. Charalambous, A. Dodd, M. McPartlin, S. O. C. Matondo, N. D. Pathirana and H. R. Powell, *Polyhedron*, 1988, **7**, 2235.
- 14 W. O. Nelson, T. B. Karpishin, S. J. Rettig and C. Orvig, *Inorg. Chem.*, 1988, **27**, 1045.
- 15 L. Simpson, S. J. Rettig, J. Trotter and C. Orvig, *Can. J. Chem.*, 1991, **69**, 893.
- 16 W. O. Nelson, T. B. Karpishin, S. J. Rettig and C. Orvig, *Can. J. Chem.*, 1988, **66**, 123.
- 17 R. C. Hider, P. D. Taylor, M. Walkinshaw, J. L. Wang and D. van der Helm, *J. Chem. Res.*, 1990, (S) 316.
- 18 M. Streater, P. D. Taylor, R. C. Hider and J. Porter, *J. Med. Chem.*, 1990, **33**, 1749.
- 19 D. J. Clevette, D. M. Lyster, W. O. Nelson, T. Rihela, G. A. Webb and C. Orvig, *Inorg. Chem.*, 1990, **29**, 667.
- 20 D. J. Clevette, W. O. Nelson, A. Nordin, C. Orvig and S. Sjoberg, *Inorg. Chem.*, 1989, **28**, 2079.
- 21 W. M. Latimer, *The Oxidation States of the Elements and their Potentials in Aqueous Solutions*, Prentice-Hall, New York, 1952.
- 22 R. C. Hider, G. Kontoghiorgos and J. Silver, *UK Pat.*, GB211 8176A, 1982.
- 23 G. M. Sheldrick, SHELX 76, A program for crystal structure determination, University of Cambridge, 1976.
- 24 G. M. Sheldrick, SHELXS 86, program for the solution of crystal structures, University of Göttingen, 1986.
- 25 C. K. Johnson, ORTEP, Report ORNL-5138, Oak Ridge National Laboratory, TN, 1965.

Received 24th February 1992; Paper 2/00968D